CrossMark

ORIGINAL RESEARCH ARTICLE

Semi-Mechanistic Model for Predicting the Dosing Rate in Children and Neonates for Drugs Mainly Eliminated by Cytochrome Metabolism

Lena Cerruti[1] · Nathalie Bleyzac[2] · Michel Tod[1,2,3,4]

Abstract

Background and Objective A simple approach is proposed to predict drug clearance in children when no paediatric data are available for drugs metabolised by cytochromes.
Methods The maturation functions of cytochrome activity and binding proteins in plasma were combined with several measures of body size to describe drug clearance increase with age. The complete model and different reduced models were evaluated on a large panel of drug clearance data in children. The parameters of the models were estimated by nonlinear regression. Bias and precision of predictions were determined.
Results Two hundred and ten clearance ratios were available for the analysis, corresponding to 53 drugs mainly eliminated by cytochrome metabolism. The age range was 1.5 day to 16 years and there were 30 values for children aged less than 2 years. Fat-free mass at power 0.75 yielded better results than the other body size descriptor tested. The model with the best fit was based on the fat-free mass ratio, the unbound fraction ratio, maturation functions for cytochromes and no maturation function for clearance by other routes. In children aged less than 2 years, the predictive performances were much better with the final model than with the model based on body surface area. The final model was almost unbiased.
Conclusions This model allows the calculation of the maintenance dose of drugs eliminated mainly by cytochromes. After external validation, it could be used in children aged less than 2 years. In older children, the model reduces to a simple approach based on body surface area or preferably on fat-free mass at power 0.75. The model is not suitable for preterm neonates.

✉ Michel Tod
michel.tod@univ-lyon1.fr

1 Pharmacie, Groupement Hospitalier Nord, Hospices Civils de Lyon, Lyon, France

2 EMR3738, Faculté de médecine Lyon-sud, Université Lyon 1, Lyon, France

3 Faculté de pharmacie, Université Lyon 1, Lyon, France

4 EMR3738, Faculté de médecine Lyon-sud, BP 12 Chemin du grand revoyet, 69921 Oullins, France

Key Points

For drugs eliminated mainly by cytochrome metabolism, clearance in children may be estimated using a simple model based on body size, unbound fraction and the contribution ratio of each cytochrome to drug clearance in adults.

This model was evaluated for 53 drugs and was almost unbiased.

This model could be especially useful for children aged less than 2 years after external validation.

1 Introduction

The maintenance dose of drugs (in mg/day) to reach a given target average concentration is lower in children than in adults because drug clearance (CL, in L/h) is lower. It

has been recognised that CL is lower because [1] body size (BS), which is correlated with the mass of eliminating organs, is smaller and [2] elimination organs are eventually immature, i.e. the elimination rate per unit of organ mass is lower than in adults [1, 2]. Correction for BS has been based either on body weight (BW), BW at power 3/4 or body surface area (BSA). There are strong theoretical reasons to support BW at power 3/4 as the best covariate for drug CL [3–5], stemming from the allometric theory. However, BSA, which is proportional to BW at power 2/3, is widely used and gives good accuracy [6].

Regarding maturation of elimination pathways, it has been found that the time course of maturation with age is well described by a sigmoidal relationship (e.g. [7, 8]). However, the parameters of the maturation function depend on the elimination pathway. Much work has been done on maturation of renal function [9, 10] and metabolism by cytochromes (CYPs) [11–13]. Some work has been done on maturation of other metabolic pathways such as conjugation [8]. In almost all cases, maturation is completed at the age of 2 years, but the time course of maturation is variable among pathways. Because competing elimination pathways do not mature at the same rate, the proportion of different pathways may vary from birth to adulthood. As a result, the metabolic fate may be different in neonates from that in adults [14], and the magnitude of drug–drug interactions may vary with age [15, 16].

Currently, data of pharmacokinetic studies in children are analysed mainly by population approaches [17–20]. When no paediatric data are available, predictions are frequently based on physiologically based pharmacokinetic models [11, 19–21], which can be considered as full mechanistic models. However, there is still a need for a simpler approach to predict drug CL and drug–drug interactions in children when no paediatric data are available, especially for drugs metabolised by CYPs. A semi-mechanistic approach was proposed by Suzuki et al. in 2010 to predict drug metabolic CL in children [22]. However, the approach was limited to drugs eliminated entirely by the liver, and the application to only four drugs was presented.

In this article, the approach of Suzuki et al. was extended by relaxing the restriction of CL exclusively by the liver. A simple model, allowing an existing database on CYP contribution to total CL to be used [23], was fitted to a large panel of paediatric studies. As a result, calculation of maintenance dose in children for drugs metabolised by CYPs is facilitated.

2 Methods

The goal of the model was to predict the ratio of drug CL (CL) in children (CL_{ch} in L/h) to drug CL in adults (CL_{ad} in L/h), according to some covariates to be determined. When the drug is administered by the intravenous route, this ratio (denoted R_{CL}) is CL_{ch}/CL_{ad}. When the drug is administered by the oral route, R_{CL} is $(CL/F)_{ch}/(CL/F)_{ad}$.

2.1 Models

Clearance in L/h is lower in children than in adults because BS is lower and elimination organs are eventually immature. To distinguish these two effects, it is convenient to write:

$$CL_{ch} = CL_{ad} \cdot \frac{BS_{ch}}{BS_{ad}} \cdot \text{Mat(age)},$$

where BS is some measure of BS (such as BSA or BW) and Mat is a maturation function that increases with age to reach a value of 1 in adults.

In this article, we focus on drugs mainly eliminated by metabolism by CYPs. The key idea is to combine the known maturation functions of CYP activity with some measure of BS to describe the CL increase with age.

First, we need to model the contribution of each CYP to the total CL in adults. We used the concept of the contribution ratio (CR), which is the fraction of total oral CL mediated by a given CYP:

$$CR_{CYP} = \frac{CL^{oral} - CL^{oral}_{-CYP}}{CL^{oral}},$$

where CL^{oral}_{-CYP} is the oral CL when the CYP is not functional (either by genetic variation or by complete inhibition by a co-medication). This concept was introduced by Ohno et al. [24]. When liver CL is equal to total CL (no other route of elimination), CR is equal to the usual parameter f_m, the fraction of drug intrinsic CL mediated by this CYP. When liver CL is less than total CL, CR is no longer equal to f_m [25]. However, the concept of CR is relevant in both cases to model the impact of maturation. The reason for choosing CR as the key parameter is that [1] its estimation is based solely on clinical data, avoiding pitfalls associated with in vitro-in vivo extrapolation and [2] it has been estimated for 200 substrates [24, 26–30] from published drug–drug interaction or pharmacogenetic studies, allowing a validation of the approach on a large panel of drugs.

For a given drug, the CR may depend on the route of administration. In particular, the CR may be smaller after intravenous administration than after oral administration because there is no first-pass effect. Hence, the difference between oral and intravenous CRs may occur for drugs with high hepatic extraction yield. However, in the rest of the article, we do not distinguish oral and intravenous CRs and we use the values of CRs obtained from oral data in all cases because no drug with a high extraction yield was given intravenously in the dataset.

Second, we need to incorporate maturation function of each CYP, i.e. the variation of the fraction of adult CYP abundance (Ab) with age, into the expression of metabolic CL. Total CL in children is decomposed as the sum of CL mediated by CYPs ($CLcyp_{ch}$) and CL by other routes ($CLother_{ch}$):

$$CL_{ch}(age) = CLcyp_{ch}(age) + CLother_{ch}(age).$$

Define S_{CR} and S_{CRab} as the sum of CRs and the Ab-corrected sum of CRs, respectively:

$$S_{CR} = \sum CR_j \text{ and } S_{CRab}(age) = \sum CR_j \cdot Ab_j(age),$$

where the sum is over all the CYPs involved in the metabolism of the drug.

Then, if there is a single CYP involved:

$$CLcyp_{ch}(age) = CLcyp_{ad} \cdot \frac{BS_{ch}}{BS_{ad}} \cdot Ab(age)$$
$$= CR \cdot CL_{ad} \cdot \frac{BS_{ch}}{BS_{ad}} \cdot Ab(age).$$

If there are several CYPs:

$$CLcyp_{ch}(age) = CL_{ad} \cdot \frac{BS_{ch}}{BS_{ad}} \cdot S_{CRab}(age) \text{ and}$$

$$CLother_{ch} = CLother_{ad} \cdot \frac{BS_{ch}}{BS_{ad}} \cdot Mat(age)$$
$$= (1 - S_{CR}) \cdot CL_{ad} \cdot \frac{BS_{ch}}{BS_{ad}} \cdot Mat(age).$$

Here, $Mat(age)$ is a maturation function (to be determined) that describes the increase of CL by other routes as a function of age. The form of the maturation function is:

$$Mat(age) = \frac{age^s}{age_{50}^s + age^s}.$$

Finally, the ratio of CLs is: $\frac{CL_{ch}}{CL_{ad}} = \frac{BS_{ch}}{BS_{ad}} \cdot [S_{CRab} + Mat(age) \cdot (1 - S_{CR})]$.

Depending on the route of administration and the extraction yield, renal and metabolic CLs are proportional, or at least correlated, with the unbound fraction of drug in plasma (fu). Because fu is higher in neonates than in adults, an empirical correction of the CL ratio by the unbound fraction ratio was also considered. Last, to adjust for an eventual bias in the model, a regression parameter R_{max} was introduced, leading to the complete model:

$$\frac{CL_{ch}}{CL_{ad}} = R_{max} \cdot \frac{BS_{ch}}{BS_{ad}} \cdot \frac{fu_{ch}}{fu_{ad}}$$
$$\cdot [S_{CRab} + Mat(age) \cdot (1 - S_{CR})].$$

The maturation functions for CYP Ab and unbound fractions are given in the "Appendix".

Regarding the choice of BS descriptor, several metrics were evaluated: BSA, BW at power 0.75, or normal fat mass (NFM) at power 0.75, which combines allometry with

an adjustment for body fat [8]. Normal fat mass separates the contributions of fat-free mass (FFM) and fat mass (BW−FFM) to drug CL:

$$NFM = FFM + F_{fat} \cdot (BW - FFM),$$

where F_{fat} is a parameter to be estimated and *FFM* is calculated from body mass index (BMI = BW/height in kg/m^2) as [31]:

$$FFM = \frac{BMI_{max} \cdot BW}{BMI_{50} + BMI}.$$

For men, $BMI_{max} = 42.92$ and $BMI_{50} = 30.93$ kg/m^2. For women, $BMI_{max} = 37.99$ and $BMI_{50} = 35.98$ kg/m^2. The complete model and different reduced models were evaluated on a large panel of drug CL data in children.

2.2 Data Collection

The data were mainly retrieved from a literature search in PubMed, using the keywords 'Drug name/pharmacokinetics'[Mesh] AND ('infant'[MeSH Terms] OR 'child'[MeSH Terms] OR 'adolescent'[MeSH Terms]). Only articles written in English or in French were considered. Articles were excluded if they considered only preterm neonates, or in the case of non-imputable missing data.

The following data were extracted: post-natal age (years), BW (kg), height (cm), drug CL (L/h) and route of administration (intravenous or oral). Missing demographic data were imputed using the Swiss growth table [32]. For example, the typical BW might be inferred from age.

The values of drug CL in adults were extracted from Goodman and Gillman [33], DrugBank [34] or from a literature search in PubMed.

Body surface area was assumed to be 1.73 m^2 in adults, while in children, BSA was calculated using the formula of Gehan and George [35], using the means of height and BW from each study:

$$BSA_{ch}(m^2) = 0.0235$$
$$\times \text{ height } (cm)^{0.42246} \times BW \ (kg)^{0.51456}.$$

Body weight in adults was assumed to be 70 kg. The NFM in adults was fixed to 42.1 kg, equivalent to a typical BW of 70 kg.

The values of drug unbound fraction in plasma in adults fu_{ad} were extracted from DrugBank or from PubMed. The CRs were taken from the website www.ddi-predictor.org [23].

2.3 Regression Methods

The parameters of the models were estimated by non-linear regression using a maximum likelihood approach. The

regression model had a single level of random effect (the residual error):

$$(R_{CL})_{obs} = (R_{CL})_{pred} \cdot (1 + \varepsilon),$$

where ε is a random variable with Student's t distribution with 3 degrees of freedom, zero mean and variance σ^2 to be estimated. This distribution decreases the impact of outliers on parameter estimation [36].

Because the BSA ratio (R_{BSA}), which was included in all models, was suspected to be prone to error (the adult value was fixed to 1.73 m^2 in all cases, which might not be true), an uncertainty about the ratio was eventually included in the model as follows:

$$(R_{BSA})_{True} = (R_{BSA})_{Calculated} \cdot (1 + \eta),$$

where $(R_{BSA})_{Calculated}$ is the ratio obtained using 1.73 m^2 as the adult value and η is a random variable with normal distribution, zero mean and standard deviation fixed to 0.15 (corresponding to a coefficient of variation of 15%). Thus, alternative models were compared, using either $(R_{BSA})_{True}$ or $(R_{BSA})_{Calculated}$ as the covariate. The same approach was applied when BW or NFM were used as the BS descriptor.

Model selection was primarily based on the likelihood ratio test in the case of nested models, or the Akaike criterion in the case of non-nested models. Other goodness-of-fit criteria were the residual plots and the variance of the residual error, which should be as low as possible.

The software NONMEM® 7.2 (Icon Dvpt Solution, Ellicott city) was used for all computations [37]. The Laplace approximation of the likelihood was used in all cases.

2.4 Predictive Performance

The predictive performance was evaluated by computing some descriptive statistics of the fold-error (FE):

$$FE = \frac{Predicted\ R_{CL}}{Observed\ R_{CL}}.$$

The statistics were the median FE and the interquartile range of FEs. The median FE is a measure of the bias of the method and a value of 1 means that there is no bias. The interquartile range of FEs is a measure of the imprecision and it should be as low as possible.

Finally, the proportion of 'good' predictions was calculated. A prediction was considered as good if the FE was between 0.5 and 2, or between 0.67 and 1.5.

3 Results

The literature search yielded 236 values of the CL ratio. Among them, 26 were excluded because the ratio was greater than 1.2. Hence, 210 values were available for the

analysis. Among the 210 values, 56 were obtained for intravenous administration. There were 53 drugs in the database. For 45 of them, the sum of CYP contributions to the oral CL (S_{CR}) was greater than 40%, i.e. most drugs were eliminated mainly by CYP metabolism. The age range was 1.5 day to 16 years and there were 30 values for children aged less than 2 years. The details of the 210 studies are shown in Table 1 of the Electronic Supplementary Material.

Model building with the set of 210 values is summarised in Table 1. In all cases, NFM at power 0.75 yielded better results than BSA and BW at power 0.75 as the BS descriptor. Hence, the results are described mainly with NFM as the BS descriptor. The model with the lowest Akaike information criterion was the so-called model 'allometric 2'. In this model, the maturation function reduces to Mat(age) = 1, i.e. there is no maturation function on CL by routes other than CYP metabolism. The point estimate of parameter F_{fat}, which describes the contribution of fat mass to the drug CL, was nearly equal to zero, and not significantly different from zero. Hence, the term $F_{fat} \cdot (BW-FFM)$ was removed from the equations, so that NFM is equal to FFM in our model. The models accounting for an uncertainty about R_{BSA} or R_{NFM} ('ortho') had a better fit than their counterpart. The plot of the predicted vs. observed CL ratio is shown in Fig. 1.

Predictive performances for the base model and the best model are shown in Table 2 (all studies) and Table 3 (studies in children aged less than 2 years). The corresponding box plots of FEs are shown in Fig. 2 (all the data) and Fig. 3 (data for children aged less than 2 years). When assessed on all studies, the predictive performances were slightly better if the uncertainty on the NFM ratio was taken into account, but the initial model performed almost as good as the final model. In particular, the bias of the predictions was almost null. In contrast, when assessed on studies in children aged less than 2 years, the predictive performances are much better with the final model than with the initial model, and taking into account the uncertainty on the NFM ratio increased the performances. The final model was almost unbiased, contrary to the initial model.

The prediction error of the final model was independent of age and S_{CRab}, as shown by the lack of trend in residual plots of FE (Fig. 4). The value of the R_{max} estimate, which should theoretically be equal to one for an unbiased model, is shown in Table 4.

The effect of age on each component of the final model (NFM ratio, fu ratio and maturation function) is illustrated in Fig. 5. A sigmoid function was fitted to the maturation data (right plot), yielding the following equation: $1.04 \times age^{0.492}/(0.035^{0.492} + age^{0.492})$, where age is in

Table 1 Model building

Model	Name	OFV	AIC	σ^a
$R_{max} \cdot Mat(age)^b$	Empirical	3.3	11.3	0.385
$R_{max} \cdot R_{BSA}$	BSA basic	−8.2	−4.2	0.361
$R_{max} \cdot R_{BSA}$	BSA ortho^c	−13.7	−9.7	0.328
$R_{max} \cdot R_{BSA}^{1.176}$	Physio 1	−3.4	0.6	0.361
$R_{max} \cdot R_{BSA} \cdot R_{fu}$	Physio 2	−2.9	1.1	0.365
$R_{max} \cdot R_{BSA} \cdot R_{fu} \cdot Mat(age)$	Mixed 1	−24.3	−16.3	0.353
$R_{max} \cdot R_{BSA} \cdot R_{fu} \cdot [S_{CRab} + (1-S_{CR})]$	Physio 3	−29.7	−25.7	0.344
$R_{max} \cdot R_{BSA} \cdot R_{fu} \cdot [S_{CRab} + (1-S_{CR})]$	Physio 3 ortho	−35.4	−31.4	0.312
$R_{max} \cdot R_{BSA}^{1.176} \cdot R_{fu} \cdot [S_{CRab} + (1-S_{CR})]$	Physio 4	−15.9	−11.9	0.350
$R_{max} \cdot R_{BSA} \cdot [S_{CRab} + (1-S_{CR})]$	Physio 3b	−21.5	−17.5	0.350
$R_{max} \cdot R_{BSA} \cdot R_{fu} \cdot [S_{CRab} + (1-S_{CR}) \cdot Mat]$	Physio 3c	−31.2	−23.2	0.343
$R_{max} \cdot R_{bw}^{0.75} \cdot R_{fu} \cdot [S_{CRab} + (1-S_{CR})]$	Allometric 1	−22.3	−18.3	0.348
$R_{max} \cdot R_{bw}^{0.75} \cdot R_{fu} \cdot [S_{CRab} + (1-S_{CR})]$	Allometric 1 ortho	−28.3	−24.3	0.316
$R_{max} \cdot R_{ffm}^{0.75} \cdot R_{fu} \cdot [S_{CRab} + (1-S_{CR})]^d$	Allometric 2	−30.9	−26.9	0.342
$R_{max} \cdot R_{ffm}^{0.75} \cdot R_{fu} \cdot [S_{CRab} + (1-S_{CR})]$	Allometric 2 ortho	−36.4	−32.4	0.311

AIK Akaike Information Criterion, *OFV* objective function value

^{a} Standard deviation of the residual error

^{b} Sigmoidal maturation function. R_{BSA}, R_{fu} and R_{bw} are the child-to-adult ratios of body surface area, unbound fraction and body weight, respectively. See text for the expressions

^{c} Estimates obtained by orthogonal regression

^{d} R_{ffm} is $(FFM_{ch}/42.1)$

years. The half-maximum value of this function is reached at 0.035 years, i.e. 13 days after birth.

4 Discussion

In this work, a simple semi-mechanistic model for the estimation of CL of drugs mainly eliminated by CYP metabolism was proposed and evaluated. Body size and maturation of metabolism were incorporated in the model. As expected, taking into account maturation improved the prediction in children aged less than 2 years. Over 2 years, R_{BS} is enough to predict R_{CL}. To minimise the impact of imprecision or uncertainty in the data, a type of orthogonal regression coupled with a robust regression approach was used. Orthogonal regression approaches the best case for estimation of predictive performances, i.e. estimation with 'true' values of the covariates, with a consistent methodology across studies and ages.

Some data (those with a CL ratio greater than 1.2) were discarded from the analysis. Because BS and CYP activity increase as a monotone function of age to reach a plateau in adults (there is no 'overshoot'), the CL ratio should theoretically never exceed a value of 1. However, in practice, when the CL ratio is calculated by using different studies (e.g. a paediatric study and an adult study made by a different team in a different setting), experimental variations may result in a CL ratio greater than 1. This is why we arbitrarily accept CL ratios until 1.2. Larger values are certainly biased. For example, different formulations of the drug, with different bioavailability, might have been used in adults and in children. Or, metabolic rates might differ between studies because ethnicity is different. Unfortunately, some experimental details are frequently lacking, thus it is not possible to determine precisely the source of bias. This is why we decided to reject the ratios greater than 1.2.

Once the CL ratio has been estimated, the dosing rate in children, e.g. in mg/day may be calculated as the dosing rate in adults $\times R_{CL}$. This method implicitly assumes that the target concentration is the same in children and in adults, which is not always true. However, if the target concentration in adults and in children are both known, the dosing rate may be refined by taking into account the ratio of target concentrations.

With our dataset, the best BS descriptor was FFM calculated with the formula of Janmahasatian et al. [31] at power 0.75. This finding is consistent with the idea that the mass of eliminating organs is better correlated with FFM than with total mass because fat is not involved in drug CL.

Using oral CRs for intravenous data was not invalidated in this study. As explained in the methods, using oral CRs for intravenous data might be an issue for drugs with high hepatic extraction yield because the CR estimated after oral administration is expected to be greater than that estimated
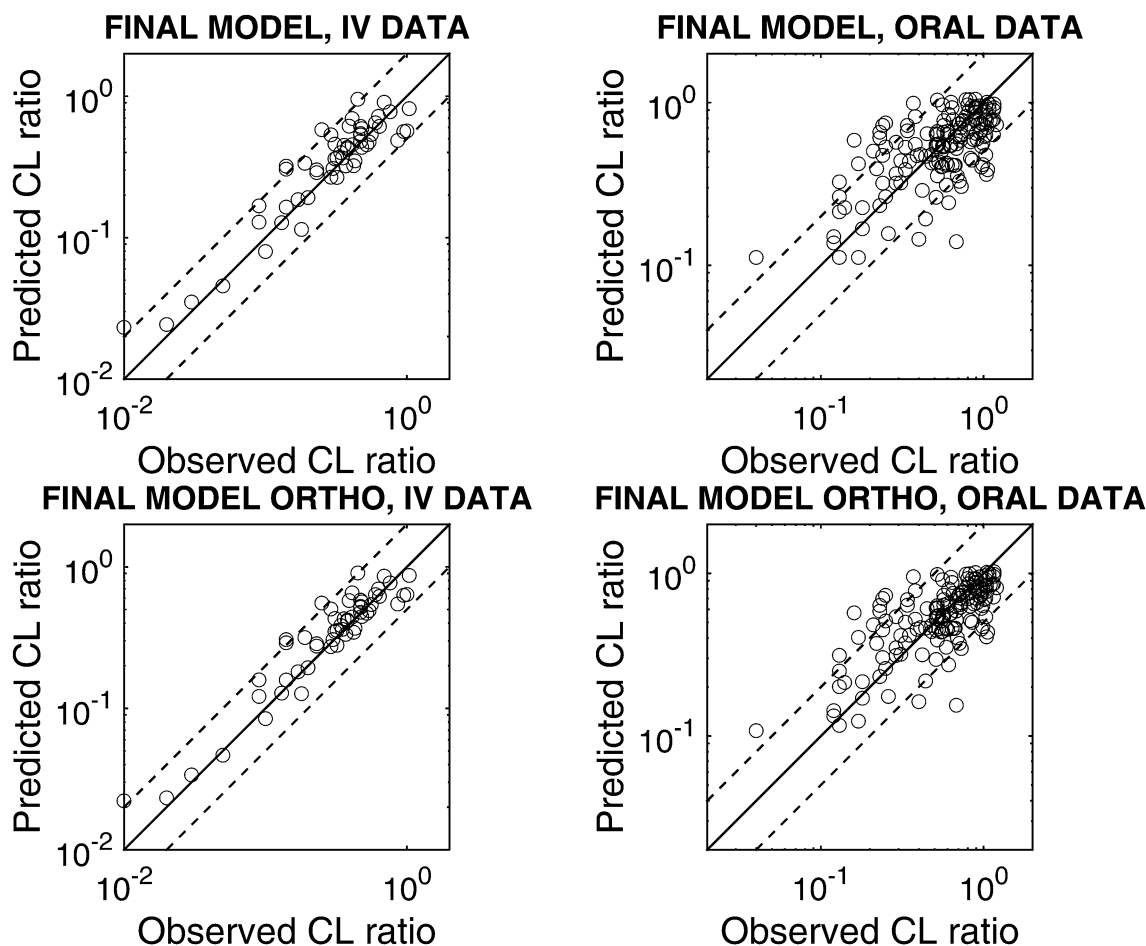
Fig. 1 Predicted vs. observed clearance (CL) ratio. Final model stands for model 'allometric 2'. *Upper range*: fat-free mass ratio assuming 42.1 kg in adults. *Lower range*: fat-free mass ratio assuming a proportional error with a coefficient of variation of 15%. *Left*: intravenous (IV) data. *Right*: oral data

Table 2 Predictive performances of the main models on 210 paediatric studies (all ages)

Model	Median FE[a]	Interquartile range FE	% within two fold	% within 1.5-fold
$R_{max} \cdot R_{BSA}$	1.01	0.59	83	64
$R_{max} \cdot R_{BSA}$ ortho[b]	1.00	0.47	87	70
$R_{max} \cdot R_{BSA} \cdot R_{fu} \cdot [S_{CRab} + (1-S_{CR})]$	1.02	0.50	84	67
$R_{max} \cdot R_{BSA} \cdot R_{fu} \cdot [S_{CRab} + (1-S_{CR})]$ ortho[b]	1.02	0.39	87	73
$R_{max} \cdot R_{bw}{}^{0.75} \cdot R_{fu} \cdot [S_{CRab} + (1-S_{CR})]$	1.03	0.52	84	66
$R_{max} \cdot R_{bw}{}^{0.75} \cdot R_{fu} \cdot [S_{CRab} + (1-S_{CR})]$ ortho[b]	1.02	0.41	86	72
$R_{max} \cdot R_{ffm}{}^{0.75} \cdot R_{fu} \cdot [S_{CRab} + (1-S_{CR})]$[c]	1.02	0.48	84	67
$R_{max} \cdot R_{ffm}{}^{0.75} \cdot R_{fu} \cdot [S_{CRab} + (1-S_{CR})]$ ortho[b]	1.02	0.37	86	73

FE fold-error

[a] FE = R_{pred}/R_{obs}

[b] Estimates obtained by orthogonal regression

[c] R_{ffm} is (FFM$_{ch}$/42.1)

after intravenous administration. However, only two drugs with high hepatic extraction were present in our dataset (buspirone and felodipine) and no intravenous data were available for them. Hence, the predictive performance of the model could not be validated for drugs with high hepatic extraction given intravenously.

Table 3 Predictive performances of the main models on 30 paediatric studies (age less than 2 years)

Model	Median FE[a]	Interquartile range FE	% within two fold	% within 1.5-fold
$R_{max} \cdot R_{BSA}$	1.28	0.92	70	50
$R_{max} \cdot R_{BSA}$ ortho[b]	1.22	0.80	77	50
$R_{max} \cdot R_{BSA} \cdot R_{fu} \cdot [S_{CRab} + (1-S_{CR})]$	1.03	0.55	73	60
$R_{max} \cdot R_{BSA} \cdot R_{fu} \cdot [S_{CRab} + (1-S_{CR})]$ ortho[b]	1.02	0.44	83	67
$R_{max} \cdot R_{bw}^{0.75} \cdot R_{fu} \cdot [S_{CRab} + (1-S_{CR})]$	0.97	0.54	77	53
$R_{max} \cdot R_{bw}^{0.75} \cdot R_{fu} \cdot [S_{CRab} + (1-S_{CR})]$ ortho[b]	0.98	0.43	80	60
$R_{max} \cdot R_{ffm}^{0.75} \cdot R_{fu} \cdot [S_{CRab} + (1-S_{CR})]$[c]	1	0.55	77	57
$R_{max} \cdot R_{ffm}^{0.75} \cdot R_{fu} \cdot [S_{CRab} + (1-S_{CR})]$ ortho[b]	1	0.43	80	67

FE fold-error

[a] $FE = R_{pred}/R_{obs}$

[b] Estimates obtained by orthogonal regression

[c] R_{ffm} is $(FFM_{ch}/42.1)$

Fig. 2 Box plot of fold-error prediction of clearance ratio, based on all data (210 values). Initial and final model stand for 'BSA basic' and 'allometric 2' model, respectively
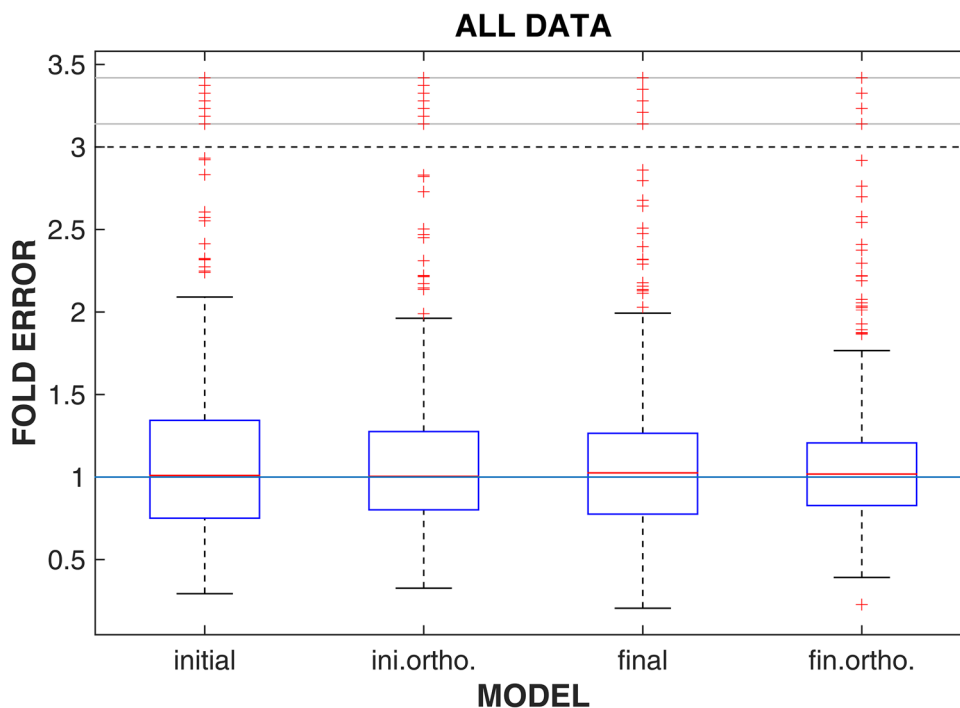
A maturation function on $(1-S_{CR})$, representing the 'non-CYP' elimination routes, was not supported by our data. If this represents renal CL, a maturation function is expected to apply. This paradoxical result might be explained by the relative paucity of data in children aged less than 2 years, and the small contribution of renal CL to total CL for the drugs considered in our study. By design, we focused on drugs eliminated mainly by CYP-mediated metabolism. If our approach was to be extended to drugs eliminated to a significant proportion by the renal route, a maturation function for renal function such as that described by Rhodin et al. [10] should certainly be included in

the model. The threshold value of S_{CR} (the sum of CRs) required to use our approach cannot be determined with the data at hand. Obviously, it depends on the nature of the non-CYP pathways, their maturation kinetics and their proportions.

Several limits of our model need to be delineated. First, the influence of disease on liver function was not taken into account. For example, inflammation may alter the expression of CYPs and transporters in the liver [38], thereby modifying drug CL, e.g. [39]. Second, our model applies only to term neonates. The same approach could be pursued for preterm neonates but more data on maturation

Fig. 3 Box plot of fold-error prediction of clearance ratio, based on data in children aged less than 2 years (30 values)
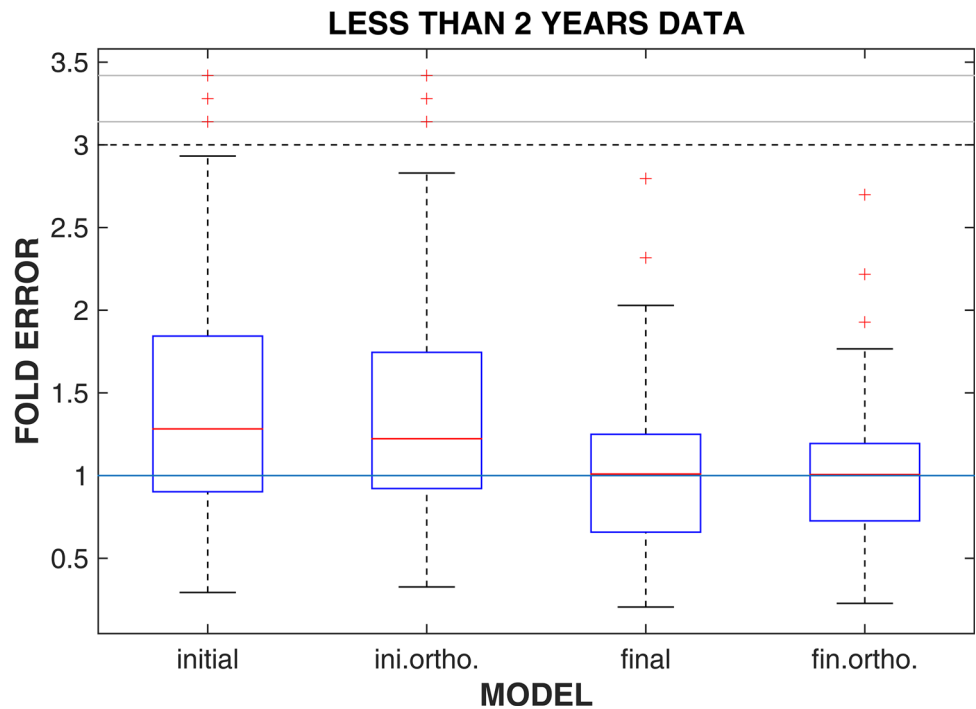

Fig. 4 Fold-error prediction of clearance ratio in children aged less than 2 years, as a function of age (*left*) or S_{CRab} (*right*). *CR* contribution ratio
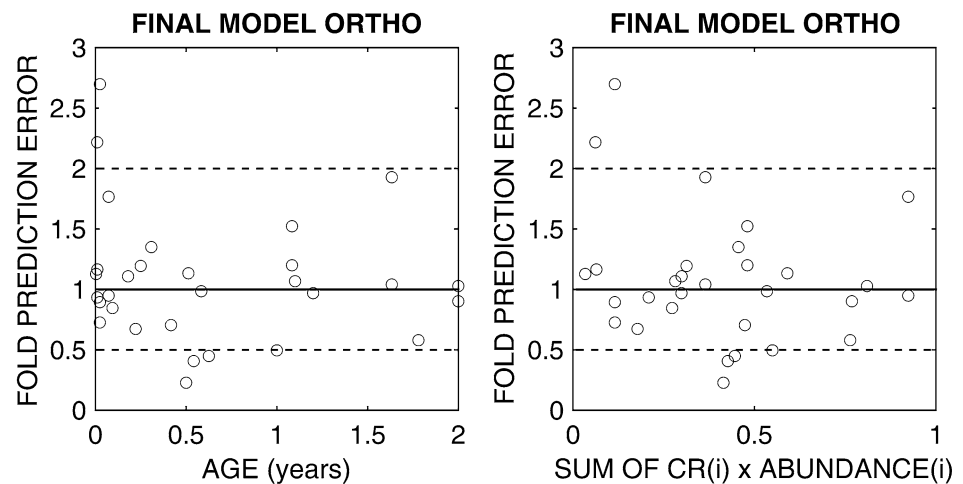

Table 4 R_{max} estimate for the main models

Model	Point estimate	RSE[b] (%)
$R_{max} \cdot R_{BSA}$	0.935	3
$R_{max} \cdot R_{BSA}$ ortho[a]	0.953	3
$R_{max} \cdot R_{BSA} \cdot R_{fu} \cdot [S_{CRab} + (1-S_{CR})]$	0.942	3
$R_{max} \cdot R_{BSA} \cdot R_{fu} \cdot [S_{CRab} + (1-S_{CR})]$ ortho	0.963	3
$R_{max} \cdot R_{bw}{}^{0.75} \cdot R_{fu} \cdot [S_{CRab} + (1-S_{CR})]$	1.1	3
$R_{max} \cdot R_{bw}{}^{0.75} \cdot R_{fu} \cdot [S_{CRab} + (1-S_{CR})]$ ortho	1.12	3
$R_{max} \cdot R_{ffm}{}^{0.75} \cdot R_{fu} \cdot [S_{CRab} + (1-S_{CR})]{}^{b}$	1.01	3
$R_{max} \cdot R_{ffm}{}^{0.75} \cdot R_{fu} \cdot [S_{CRab} + (1-S_{CR})]$ ortho	1.03	3

RSE relative standard error

[a] Estimates obtained by orthogonal regression

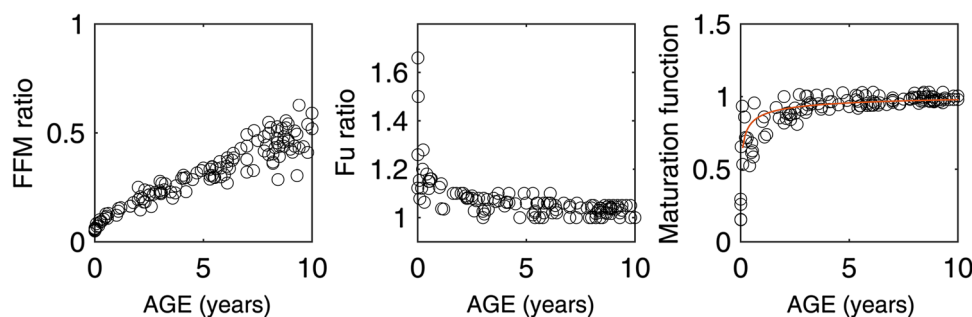[b] R_{ffm} is $(FFM_{ch}/42.1)$

Fig. 5 Variation of each component of the final model as a function of age: fat-free mass (FFM) ratio is $FFM_{ch}/42.1$, where FFM_{ch} is calculated according to [31]; unbound fraction of drug in plasma (fu) ratio is fu_{ch}/fu_{ad}, where fu_{ch} is calculated according to [11] (see "Appendix") and 'maturation function' is $S_{CRab} + (1-S_{CR})$. The *red line* is a fitted sigmoid function (see text). Each *point* represents a study (one of the 210 values used as data)

functions are needed. Prematurity is associated with lower enzyme activity, leading to a lower CL ratio and lower dosing rate. Third, our model focuses on the prediction of CL, allowing the maintenance dose to be estimated. Calculation of a loading dose would require an estimate of the volume of distribution. Fourth, the obese child is a special case that we were unable to assess with the data at hand. However, the use of FFM as a BS descriptor in our model should theoretically ensure good predictive performances in obese children [2]. Finally, linear kinetics is a necessary assumption in the calculation of CRs. Non-linear kinetics results in a variation of CRs with dosing rate.

Regarding children aged less than 2 years, there are additional limits. First, there is a paucity of data in this age range. Second, the two major components of our approach, namely the maturation functions and the CRs, are prone to uncertainty. The maturations functions published in 2006 and used in the physiologically based pharmacokinetic software package Simcyp (Certara, Princeton, NJ, USA) [11] rely on scarce data in children aged less than 2 years, and part of them were obtained in vitro. The CRs have been published since 2007 [24] and validated for prediction of the impact of CYP-mediated drug–drug interactions and genetic polymorphisms on more than 1000 examples in adults [23]. However, in neonates, some compensation (i.e. increased elimination rate per unit of tissue mass) of the low activity of CYPs by other routes may occur, resulting in a larger than expected variation of the CRs. Because of these limits, the model should be used with caution in children aged less than 2 years until an external validation has been carried out.

The model opens the way for predicting CYP-mediated drug–drug interactions and the impact of CYP polymorphisms in children aged less than 2 years within the same modelling paradigm. A consequence of the model is that the CR of the j-th CYP involved in drug metabolism in a child is:

$$CR_{ch_j}(age) = \frac{CR_{ad_j} \cdot Ab_j(age)}{\left[\sum CR_{ad_j} \cdot Ab_j(age)\right] + \left(1 - \sum CR_{ad_j}\right)},$$

where the sum is over all CYPs involved. This age-adjusted CR may be used in static models published earlier for calculation of an area under the curve ratio in the case of a drug–drug interaction or CYP polymorphism [40].

5 Conclusions

The proposed model is expected to be useful to calculate the maintenance dose of drugs eliminated mainly by CYPs. After a suitable external validation, it could be used in children aged less than 2 years. In older children, the model reduces to a simple approach based on BSA or preferably on FFM at power 0.75.

Appendix

Fraction of Cytochrome Abundance

The fraction of cytochrome (CYP) abundance with respect to the adult value as a function age was calculated using the relationships described by Johnson et al. [11], where age is in years.

For CYP1A2: $Ab = \frac{age^{1.41}}{1.13 + age^{1.41}}$

For CY2D6: $Ab = \frac{1.01\,age}{0.101+age} + 0.036$

For CYP2C9: $Ab = \frac{0.821\,age}{0.01+age} + 0.21$

For CYP2C19: $Ab = \frac{0.857\,age}{0.99+age} + 0.23$

For CYP3A4: $Ab = \frac{age^{0.83}}{0.31+age^{0.83}}$

Unbound Fractions

The unbound fractions in children were calculated as described by Johnson [11]:

$$fu_{ch} = \frac{1}{1 + \frac{(1-fu_{ad})\cdot P_{ch}}{fu_{ch}\cdot P_{ad}}},$$

where P_{ch} and P_{ad} are the concentrations of the binding protein in plasma in children and in adults, respectively.

If the binding protein is albumin, then $P_{ad} = 45$ g/L and

$P_{ch} = 1.1287 \times \mathrm{Ln}(age) + 33.746.$

If the binding protein is acid alpha-1 glycoprotein, then $P_{ad} = 0.83$ g/L and

$$P_{ch} = \frac{0.887.age^{0.38}}{8.89^{0.38} + age^{0.38}}.$$

In the two last equations, age is in days. Finally, if the binding protein is unknown, P_{ad} and P_{ch} are calculated as the mean of the two equations above.

References

1. Anderson BJ, Holford NH. Mechanism-based concepts of size and maturity in pharmacokinetics. Annu Rev Pharmacol Toxicol. 2008;48:303–32.
2. Anderson BJ, Holford NH. Understanding dosing: children are small adults, neonates are immature children. Arch Dis Child. 2013;98(9):737–44.
3. West GB, Brown JH, Enquist BJ. A general model for the origin of allometric scaling laws in biology. Science. 1997;276(5309):122–6.
4. West GB, Brown JH, Enquist BJ. The fourth dimension of life: fractal geometry and allometric scaling of organisms. Science. 1999;284(5420):1677–9.
5. West GB, Brown JH, Enquist BJ. A general model for ontogenetic growth. Nature. 2001;413(6856):628–31.
6. Crawford JD, Terry ME, Rourke GM. Simplification of drug dosage calculation by application of the surface area principle. Pediatrics. 1950;5(5):783–90.
7. Tod M, Lokiec F, Bidault R, De Bony F, Petitjean O, Aujard Y. Pharmacokinetics of oral acyclovir in neonates and in infants: a population analysis. Antimicrob Agents Chemother. 2001;45(1):150–7.
8. Anderson BJ, Holford NHG. Mechanistic basis of using body size and maturation to predict clearance in humans. Drug Metab Pharmacokinet. 2009;24(1):25–36.
9. Anderson BJ, Allegaert K, Van den Anker JN, Cossey V, Holford NH. Vancomycin pharmacokinetics in preterm neonates and the prediction of adult clearance. Br J Clin Pharmacol. 2007;63(1):75–84.
10. Rhodin MM, Anderson BJ, Peters AM, Coulthard MG, Wilkins B, Cole M, et al. Human renal function maturation: a quantitative description using weight and postmenstrual age. Pediatr Nephrol. 2009;24(1):67–76.
11. Johnson TN, Rostami-Hodjegan A, Tucker GT. Prediction of the clearance of eleven drugs and associated variability in neonates, infants and children. Clin Pharmacokinet. 2006;45(9):931–56.
12. Allegaert K, Holford N, Anderson BJ, Holford S, Stuber F, Rochette A, et al. Tramadol and o-desmethyl tramadol clearance maturation and disposition in humans: a pooled pharmacokinetic study. Clin Pharmacokinet. 2015;54(2):167–78.
13. Ince I, de Wildt SN, Wang C, Peeters MY, Burggraaf J, Jacqz-Aigrain E, et al. A novel maturation function for clearance of the cytochrome P450 3A substrate midazolam from preterm neonates to adults. Clin Pharmacokinet. 2013;52(7):555–65.
14. de Wildt SN. Profound changes in drug metabolism enzymes and possible effects on drug therapy in neonates and children. Expert Opin Drug Metab Toxicol. 2011;7(8):935–48.
15. Salem F, Johnson TN, Barter ZE, Leeder JS, Rostami-Hodjegan A. Age related changes in fractional elimination pathways for drugs: assessing the impact of variable ontogeny on metabolic drug-drug interactions. J Clin Pharmacol. 2013;53(8):857–65.
16. Salem F, Rostami-Hodjegan A, Johnson TN. Do children have the same vulnerability to metabolic drug-drug interactions as adults? A critical analysis of the literature. J Clin Pharmacol. 2013;53(5):559–66.
17. Tod M, Jullien V, Pons G. Facilitation of drug evaluation in children by population methods and modelling. Clin Pharmacokinet. 2008;47(4):231–43.
18. Zisowsky J, Krause A, Dingemanse J. Drug development for pediatric populations: regulatory aspects. Pharmaceutics. 2010;2(4):364–88.
19. Edginton AN, Schmitt W, Voith B, Willmann S. A mechanistic approach for the scaling of clearance in children. Clin Pharmacokinet. 2006;45(7):683–704.
20. Edginton AN, Schmitt W, Willmann S. Development and evaluation of a generic physiologically based pharmacokinetic model for children. Clin Pharmacokinet. 2006;45(10):1013–34.
21. Abduljalil K, Jamei M, Rostami-Hodjegan A, Johnson TN. Changes in individual drug-independent system parameters during virtual paediatric pharmacokinetic trials: introducing time-varying physiology into a paediatric PBPK model. AAPS J. 2014;16(3):568–76.
22. Suzuki S, Murayama Y, Sugiyama E, Hirunpanich V, Saito K, Sekiyama M, et al. Estimating pediatric doses of drugs metabolized by cytochrome P450 (CYP) isozymes, based on physiological liver development and serum protein levels. Yakugaku Zasshi. 2010;130(4):613–20.
23. Tod M. DDI Predictor [updated 2016/03/20/]. Available from: http://www.ddi-predictor.org/. Accessed 29 Aug 2017.
24. Ohno Y, Hisaka A, Suzuki H. General framework for the quantitative prediction of CYP3A4-mediated oral drug interactions based on the AUC increase by coadministration of standard drugs. Clin Pharmacokinet. 2007;46(8):681–96.
25. Hisaka A, Ohno Y, Yamamoto T, Suzuki H. Theoretical considerations on quantitative prediction of drug-drug interactions. Drug Metab Pharmacokinet. 2010;25(1):48–61.
26. Castellan AC, Tod M, Gueyffier F, Audars M, Cambriels F, Kassai B, et al. Quantitative prediction of the impact of drug interactions and genetic polymorphisms on cytochrome P450 2C9 substrate exposure. Clin Pharmacokinet. 2013;52(3):199–209.
27. Gabriel L, Tod M, Goutelle S. Quantitative prediction of drug interactions caused by CYP1A2 inhibitors and inducers. Clin Pharmacokinet. 2016;55(8):977–90.

28. Goutelle S, Bourguignon L, Bleyzac N, Berry J, Clavel-Grabit F, Tod M. In vivo quantitative prediction of the effect of gene polymorphisms and drug interactions on drug exposure for CYP2C19 substrates. AAPS J. 2013;15(2):415–26.

29. Loue C, Tod M. Reliability and extension of quantitative prediction of CYP3A4-mediated drug interactions based on clinical data. AAPS J. 2014;16(6):1309–20.

30. Tod M, Goutelle S, Clavel-Grabit F, Nicolas G, Charpiat B. Quantitative prediction of cytochrome P450 (CYP) 2D6-mediated drug interactions. Clin Pharmacokinet. 2011;50(8):519–30.

31. Janmahasatian S, Duffull SB, Ash S, Ward LC, Byrne NM, Green B. Quantification of lean bodyweight. Clin Pharmacokinet. 2005;44(10):1051–65.

32. Braegger C, Jenni O, Konrad D, Molinari L. Courbes de croissance pour la Suisse. Zurich: Société Suisse de Pédiatrie. 2012.

33. Brunton L, Chabner BA, Knollman B. Goodman and Gilman's: the pharmacological basis of therapeutics. 12th edn. New-York: Mc Graw-Hill Companies; 2011.

34. Knox C, Law V, Jewison T, Liu P, Ly S, Frolkis A, et al. DrugBank 3.0: a comprehensive resource for 'omics' research on drugs. Nucleic Acids Res. 2011;39(Database issue):D1035–41.

35. Gehan EA, George SL. Estimation of human body surface area from height and weight. Cancer Chemother Rep. 1970;54(4):225–35.

36. Dosne AG, Bergstrand M, Karlsson MO. A strategy for residual error modeling incorporating scedasticity of variance and distribution shape. J Pharmacokinet Pharmacodyn. 2016;43(2):137–51.

37. Beal S, Sheiner LB, Boeckmann A, Bauer RJ. NONMEM user's guides. Ellicott City (MD); Icon Development Solutions; 2009.

38. Klein M, Thomas M, Hofmann U, Seehofer D, Damm G, Zanger UM. A systematic comparison of the impact of inflammatory signaling on absorption, distribution, metabolism, and excretion gene expression and activity in primary human hepatocytes and HepaRG cells. Drug Metab Dispos. 2015;43(2):273–83.

39. Veringa A, Ter Avest M, Span LF, van den Heuvel ER, Touw DJ, Zijlstra JG, et al. Voriconazole metabolism is influenced by severe inflammation: a prospective study. J Antimicrob Chemother. 2017;72(1):261–7.

40. Tod M, Nkoud-Mongo C, Gueyffier F. Impact of genetic polymorphism on drug-drug interactions mediated by cytochromes: a general approach. AAPS J. 2013;15(4):1242–52.